

**Clusterization of self-propelled particles in a two-component system**Shibashis Paul,<sup>1</sup> Debankur Bhattacharyya,<sup>2,\*</sup> and Deb Shankar Ray<sup>1,†</sup><sup>1</sup>*Indian Association for the Cultivation of Science, Jadavpur, Kolkata 700032, India*<sup>2</sup>*Indian Institute of Technology Kharagpur, Kharagpur, West Bengal 721302, India*

(Received 19 June 2019; revised manuscript received 20 November 2019; published 29 January 2020)

We consider a mixture of active solute molecules in a suspension of passive solvent particles comprising a thermal bath. The solute molecules are considered to be extended objects with two chemically distinct heads, one head of which having chemical affinity towards the solvent particles. The coupled Langevin equations for the solvent particles along with the equations governing the dynamics of active molecules are numerically simulated to show how the active molecules self-assemble to form clusters which remain in dynamic equilibrium with the free solute molecules. We observe an interesting crossover at an intermediate time in the variation of the order parameter with time when the temperature of the bath is changed signifying the differential behavior of clusterization below and above the crossover time associated with a transition between a thermodynamic and a quasithermodynamic regime. Enthalpy-entropy compensation in the formation of clusters below the crossover is demonstrated.

DOI: [10.1103/PhysRevE.101.012611](https://doi.org/10.1103/PhysRevE.101.012611)**I. INTRODUCTION**

An assembly of particles which draw energy at the individual level from the surroundings to execute self-propelled coordinated motion constitutes what is referred to as active matter [1–11]. The subject encompasses a variety of systems, e.g., bird flocks [12], fish schools [13], insect swarms [14], migrating bacteria [15], molds [16], and pedestrians [17]. Over the years both discrete [1,7,18] as well as continuum models based on hydrodynamics [3–5,8,19] have been proposed to investigate the universal features of collective behavior [8], new phase transitions [1,2], structure-forming cytoskeletons of cells [20], controlling liquid crystals swirling on spherical vesicles [21], modeling of tissues and tumors as flowing cells self-organizing through cell-to-cell short range interaction [22,23], homochirality in chemical systems [24], and pattern formation in activator-inhibitor systems [25] to name a few.

A key feature of the self-propelled coordinated motion of particles in active matter is that it concerns systems under far-from-equilibrium condition. More specifically, the symmetry-breaking transition between a disordered and an ordered state is affected by external noise on the particles the motion of which is governed by a mean speed and an alignment determined by that of their neighboring particles within a sphere of interaction assisted by small fluctuations [1,7]. As the motion of the particles in discrete time steps follows simple local interaction rules without any specific form of potential, the statistical approach captures many realistic features in flocking behavior, which has been complemented by the detailed consideration of hydrodynamic approaches. The

focus of the present paper is to explore the collective behavior of active systems undergoing clusterization, in a thermal bath of solvent particles. The active systems are considered to be molecules or extended objects with two heads, one head having chemical affinity towards the solvent particles. Our model of a two-component system is mainly motivated by the experimental and theoretical work on active colloidal suspensions [26–29] pioneered by Wu and Libchaber [30]. Theurkauff *et al.* [31] have experimentally investigated the collective behavior of a dense active suspension of gold colloids half covered with platinum which are spherical Janus particles [32–38] undergoing self-phoretic motion on consumption of hydrogen peroxide to exhibit a novel cluster phase at high densities. At low densities, as observed by Howse *et al.* [39], colloidal particles use chemical reaction catalyzed on their own surface to achieve directed motion. The nonequilibrium steady state of an active colloidal suspension under gravity has been investigated by Palacci *et al.* [40] to introduce the concept of an effective temperature of the active system in the light of the fluctuation-dissipation relationship. Active hydrodynamics has also been studied by Miño *et al.* [41] to understand enhanced diffusion at a solid surface. The common feature of all these colloidal suspensions is that they are, in general, two-component systems, composed of an active system and a passive solvent. The activity leading to self-propulsion is affected by chemical or other means. Based on these considerations we introduce a two-component system with an active solute and a passive solvent modeled as a thermal bath. This naturally concerns Brownian noise of the thermal bath and furthermore we consider solvent-induced interaction due to the affinities between one head of the solute molecules towards solvent particles. The dynamics of solvent particles is treated by Langevin equations while the motion of the solute molecules is guided by a scaled mean speed as determined by the Brownian motion. The activity of the solute molecules in this model originates from their

\*Present address: University of Maryland, College Park, MD 20742, USA.

†Corresponding author: [pcdsr@iacs.res.in](mailto:pcdsr@iacs.res.in)

tendency to align themselves in the close vicinity of the solvent particles within an interaction region. In other words, while the magnitude of the self-propelled velocities of the solute molecules originates from thermal motion of the bath, their directions are self-regulated due to their chemical affinity towards solvent particles. The approach is thus a synthesis of Brownian dynamics controlled by internal noise obeying the fluctuation-dissipation relation and active dynamics governed by external noise without taking into consideration explicit interaction potentials as considered by several authors [42–44]. We show that starting from a homogeneous, symmetric state the time evolution of the dynamics leads to a symmetry-broken state, i.e., a state of clusters which remains in dynamic equilibrium with free solute molecules. To characterize the transition between the homogeneous and the clustered state we introduce an order parameter in terms of the number of active solute molecules inside the interaction region. A key observation is the crossover of the order parameter at an intermediate time when the temperature of the bath is varied signifying the differential behavior of clusterization below and above the crossover. We also examine the aspects of dynamic clustering in the context of variation of interaction range and density. Finally the temperature dependence of clusterization is used to estimate the enthalpy and entropy of the formation of self-assembly below the crossover to demonstrate the approximate linearity of the enthalpy-entropy plot, signifying that the entropy effect due to repulsive interaction within the interaction region roughly balances the enthalpy effect originating from the attractive interaction due to the affinity of the solvent particles towards one head of the solute molecules.

Before leaving this section it is pertinent to discuss the similarity of the strategy employed here with that of multiparticle collision dynamics (MPCD) [45–48], which has been widely used in the context of dynamics of vesicles in shear flow [45], polymer dynamics [48], and hydrodynamic flow in presence of colloidal particles [46]. The MPCD simulation technique is primarily based on two steps. In the first streaming step the particles are allowed to move ballistically with a velocity which is used to update the position of the particle in time. In the collision step one considers stochastic rotation of the relative velocity of each particle located inside the cell. In order to include the effect of colloidal suspensions one has to introduce excluded volume interaction in the dynamics [46]. For fluid vesicles in a shear flow [45] one has to combine MPCD with the dynamically triangulated membrane model. While the MPCD bears some similarity with the present scheme since in both of them the position of the particle is updated by a ballistic step, the basic difference lies in the updating of velocity in two cases. In MPCD one uses external noise whereas in the present scheme internal noise is used so that the passive particles are thermally equilibrated and the speed used for updating position is thermal in nature. The speed of a solute molecule which executes active motion is determined by scaled thermal motion of the solvent particles. Its position is governed by relative fluctuation of population of solvent particles in its neighborhood whereas its orientation is determined by an external noise in the spirit of the Vicsek model. Unlike the present case the treatment of interaction with colloidal particles, polymer, or vesicle with MPCD depends on the specific situation.

The plan of the paper is as follows. In the next section we introduce the model with discrete dynamics for the two-component system and an order parameter to characterize the symmetry-breaking transition. The results of numerical simulations are discussed in Sec. III. The enthalpy-entropy compensation is examined in Sec. IV. The paper is concluded in Sec. V.

## II. A DISCRETE MODEL FOR CLUSTERIZATION IN TWO DIMENSIONS

To study the clusterization of self-propelled molecules we consider a model two-component solute-solvent system. The solvent particles comprising a bath at a characteristic temperature  $T$  undergo Brownian movement due to thermal fluctuations. The solute molecules on the other hand are assumed to be extended objects each with a head which has some characteristic affinity towards the solvent particles when they come close to each other. These locally interacting solute molecules with an intrinsic driving force in the close vicinity of solvent particles are characterized by velocities the magnitude of which is governed by a scaled mean speed of the solvent particles while their directions are self-regulated due to the local interaction as well as weak external noise. The model therefore essentially portrays the combined motion of Brownian dynamics of solvent particles and the self-propelled active motion of solute molecules as the conspicuous feature of clusterization.

### A. The scheme

We consider a solvent-solute model consisting of  $N_C$  number of solvent particles ( $C$ ) and  $N_{A-B}$  number of solute molecules ( $A - B$ ) moving in a two-dimensional square box with sides  $L$  and under periodic boundary condition. The solvent particles are characterized by their location  $\vec{r}_C(i)$  [with Cartesian components  $x_C(i)$  and  $y_C(i)$ ] and velocity  $\vec{v}_C(i)$  [with Cartesian components  $v_C^x(i)$  and  $v_C^y(i)$ ]. Since the molecule  $A - B$  is an extended object with a head  $A$  and the remaining extension with its head as  $B$ , for a given position of  $A$ , the head  $B$  can be located on a circle. We therefore denote  $\vec{r}_A(i)$  [with Cartesian components  $x_A(i)$  and  $y_A(i)$ ] for the position vector of the head  $A$  and  $\vec{r}_B(i)$  [with Cartesian components  $x_B(i)$  and  $y_B(i)$ ] for the position vector of the head  $B$  for the remaining part of the molecule  $A - B$ .

We now begin with the dynamics of solvent particles  $C$ . They undergo Brownian motion described by a Langevin equation for each particle. The location of the  $i$ th particle can be updated componentwise at each time step as

$$x_C(i, t + \Delta t) = x_C(i, t) + v_C^x(i, t + \Delta t)\Delta t, \quad (2.1)$$

$$y_C(i, t + \Delta t) = y_C(i, t) + v_C^y(i, t + \Delta t)\Delta t \quad (2.2)$$

where the velocity components  $v_C^x(i, t + \Delta t)$  and  $v_C^y(i, t + \Delta t)$  are given by

$$v_C^x(i, t + \Delta t) = v_C^x(i, t) + [-\gamma v_C^x(i, t)\Delta t + \xi_x(i, t)\sqrt{\Delta t}], \quad (2.3)$$

$$v_C^y(i, t + \Delta t) = v_C^y(i, t) + [-\gamma v_C^y(i, t)\Delta t + \xi_y(i, t)\sqrt{\Delta t}]. \quad (2.4)$$

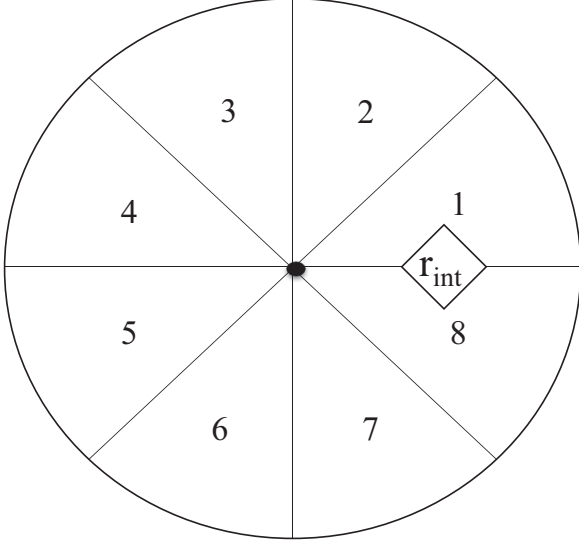


FIG. 1. The circular space of radius  $r_{\text{int}}$  around the head  $A$  of a single solute molecule, where the numbers denote the indices of the quadrants.

Here  $\gamma$  refers to the linear damping coefficient.  $\vec{\xi}(i, t)$  with components  $\xi_x(i, t)$  and  $\xi_y(i, t)$  is the Gaussian white noise with zero mean and variance  $\langle \xi_m(i, t) \xi_n(i, t') \rangle = \delta(t - t') \delta_{mn}$ .  $\xi_x(i, t)$  and  $\xi_y(i, t)$  are appropriately normalized by the strength of noise  $\sigma = \gamma k_B T$ , where  $k_B$  and  $T$  denote the Boltzmann constant and temperature, respectively. For the sake of brevity we have considered the mass of the solvent molecules to be unity. As described the solvent particles constitute a thermal bath at a given temperature.

The solute molecules  $A - B$ , on the other hand, execute self-propelled motion. This self-propelled nature of the molecules can be characterized by keeping the magnitude of mean speed  $v_0^{A-B}$  at some fixed value. In our model, we consider  $v_0^{A-B}$  to be proportional to the root mean square velocity of the solvent particles ( $v_{\text{rms}}^C$ ), where  $v_0^{A-B}$  is given by  $v_0^{A-B} = \frac{v_{\text{rms}}^C}{\kappa}$ , where  $\kappa$  is the ratio of the square root of the solute mass to solvent mass. The value of ratio  $\kappa$  is taken to be 20 throughout the simulations. For simplicity, we consider the dynamics of head  $A$  and the constrained dynamics of the remaining part with a head  $B$  separately. The solute molecules and solvent particles interact through a local rule as follows. We first locate the  $A$  head of  $A - B$  for the  $j$ th molecule and draw a circle of radius  $r_{\text{int}}$  around it as the radius of interaction with  $A$  at its center. We then divide the circle into several (say, eight) equal quadrants as shown in Fig. 1. The number of solvent particles ( $C$ ) in each quadrant is estimated. At each time step the  $A$  head of the  $j$ th molecule  $A - B$  moves to the quadrant with maximum number of solvent particles  $C$ . This is described by the equation of motion for the  $j$ th molecule as

$$x_A(j, t + \Delta t) = x_A(j, t) + v_0^{A-B} \cos \left\{ (2\nu_{\text{max}} - 1) \frac{\pi}{8} \right\} \Delta t, \quad (2.5)$$

$$y_A(j, t + \Delta t) = y_A(j, t) + v_0^{A-B} \sin \left\{ (2\nu_{\text{max}} - 1) \frac{\pi}{8} \right\} \Delta t. \quad (2.6)$$

Here  $\nu_{\text{max}}$  is the index of the quadrant with maximum number of  $C$  particles. Thus, in our model the dynamics of the solute molecules is guided by the self-propulsion of the solute heads  $A$ , and consequent placing of the  $B$  head on any random point on the circumference of a circle centring around head  $A$  with a radius  $r_{A-B}$  for the corresponding time step. The location of the  $B$  head of the solute molecule  $A - B$  is given by

$$x_B(j, t + \Delta t) = x_A(j, t + \Delta t) + r_{A-B} \cos \{2\pi R_B(j, t + \Delta t)\}, \quad (2.7)$$

$$y_B(j, t + \Delta t) = y_A(j, t + \Delta t) + r_{A-B} \sin \{2\pi R_B(j, t + \Delta t)\} \quad (2.8)$$

where  $R_B$  denotes a real-valued random number uniformly distributed between 0 and 1. Because of the finite size of the  $A - B$  solute molecules it is further necessary to put a restriction on the number of molecules ( $N_{\text{threshold}}$ ) forming a cluster within the interaction radius  $r_{\text{int}}$ . If the number of  $A - B$  molecules is higher than  $N_{\text{threshold}}$ , the additional one will have to be relocated randomly outside the circle.

In order to carry out numerical simulation of the dynamics of solute-solvent interaction, it is necessary to specify the initial conditions. Since they span the  $L \times L$  square box uniformly we assign the initial distribution of  $A - B$  and  $C$  as follows. For solvent particles ( $C$ )

$$x_C(i) = R_C^x(i)L, \quad y_C(i) = R_C^y(i)L. \quad (2.9)$$

For solute molecules ( $A - B$ )

$$x_A(j) = R_A^x(j)L, \quad y_A(j) = R_A^y(j)L, \quad (2.10)$$

$$\begin{aligned} x_B(j) &= x_A(j) + r_{A-B} \cos[2\pi R_B(j)], \\ y_B(j) &= y_A(j) + r_{A-B} \sin[2\pi R_B(j)]. \end{aligned} \quad (2.11)$$

Here  $R_C^x(i)$ ,  $R_C^y(i)$ ,  $R_A^x(j)$  and  $R_A^y(j)$  are independent real valued random numbers uniformly distributed between 0 and 1. The index  $i$  runs for solvent particles ( $C$ ) from 1 to  $N_C$  and  $j$  runs for solute molecules ( $A - B$ ) from 1 to  $N_{A-B}$ .  $N_C$  and  $N_{A-B}$  are total number of solvent particles and solute molecules, respectively.  $r_{A-B}$  stands for the “length” of the solute molecule  $A - B$ .

Keeping in view these considerations a remark on the time scales of solute molecules and solvent particles is in order. We emphasize that since the stochastic motion of passive solvent particles is due to the thermal bath kept at a constant temperature, the Langevin noise [Eqs. (2.1)–(2.4)] being internal, the time scale is determined by translational diffusion. The solute molecule which is assumed to have a physical extension is characterized by a mass much larger than that of a solvent particle. For translational motion or mean motion of solute molecules we therefore use a constant speed appropriately scaled by the ratio of the square root of solute to solvent mass. Its position is updated by this speed and density of solvent particles in the neighborhood. The orientation of the solute molecule is, however, governed by an external noise. Thus the rotational time scale of solute molecules is determined by the active noise [Eqs. (2.7) and (2.8)], which is external in origin and thus bears a close kinship with the Vicsek model of self-propelled dynamics in active media. Finally, a caveat to

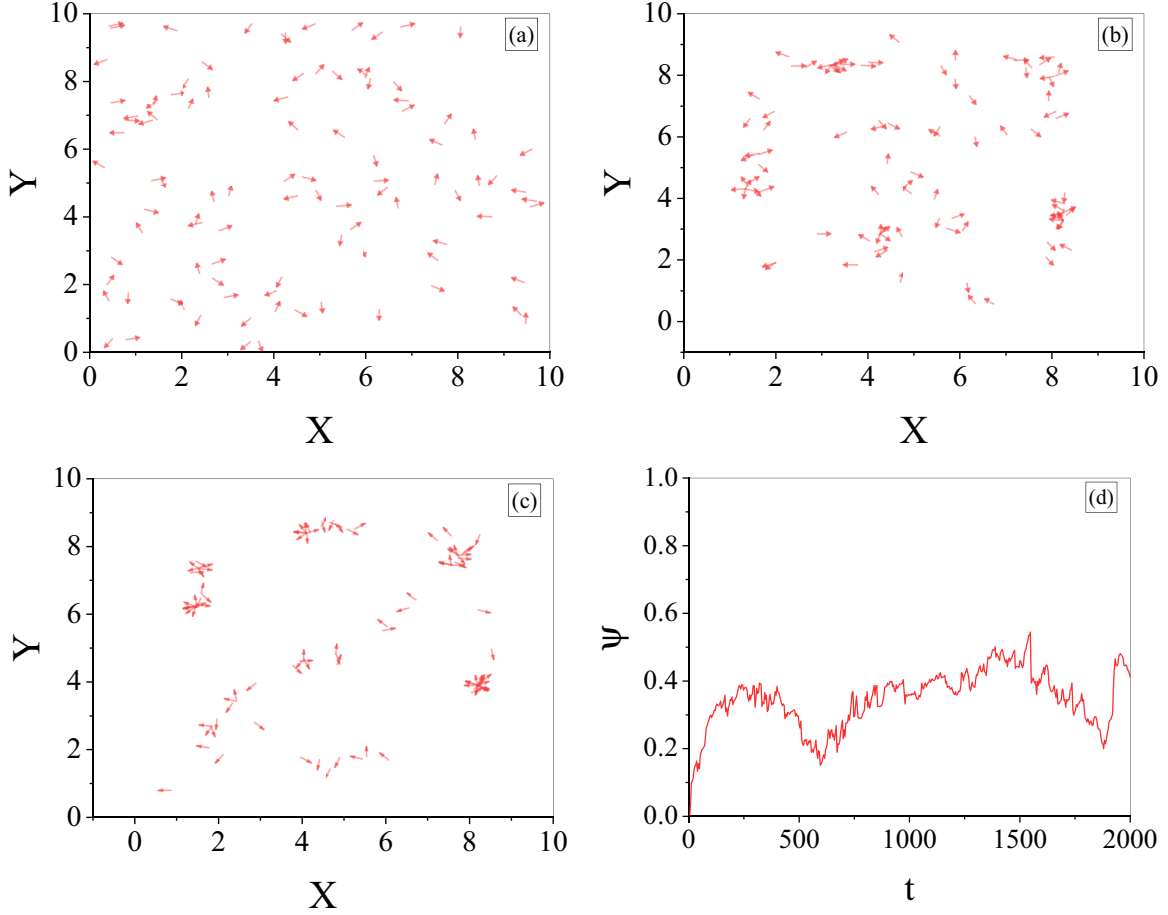


FIG. 2. The spatiotemporal profile of the solute molecules (solvent particles not shown) simulated with the following parameter values:  $r_{\text{int}} = 2.0$ ,  $r_{A-B} = 0.3$ ,  $L = 10.0$ ,  $\gamma = 0.5$ ,  $k_B = 1.0$ ,  $T = 1.0$ ,  $N_{A-B} = 100$ ,  $N_C = 1000$ ,  $N_{\text{threshold}} = 20$ ,  $\Delta t = 0.005$  at (a)  $t = 0$ , (b)  $t = 1000$ , and (c)  $t = 2000$  time units, respectively. (d) Variation of the order parameter of the system with respect to time for the same simulation (units arbitrary).

note is that the Vicsek model is nonthermal while our model is quasithermal in character since we are concerned with active solutes in passive Brownian solvent.

In summary, the dynamics of the solute-solvent interaction is such that solvent particles forming a thermal bath are responsible for imparting an average speed to the solute particles which execute self-coordinated motion by aligning their heads towards the solvent particles. In what follows we show that the evolution of dynamics leads to the emergence of a cluster phase.

### B. The order parameter

The dynamics of solute-solvent interaction is governed by an interplay of the Brownian motion of solvent particles constituting a thermal bath at a temperature  $T$  and the self-propelled or active motion of solute molecules. The interaction proceeds in such a way that the specific heads of the solute molecules undergo flocking around the solvent molecules within a range of interaction leading to clusterization of finite size. This clusterization is controlled by local interaction and an intrinsic driving force causing symmetry breaking in the system.

For the statistical characterization of the associated symmetry breaking and clusterization, we now introduce an order parameter  $\psi$  as follows:

$$\psi = \frac{\langle N_{r_{\text{int}}}(t) \rangle - \langle N_{r_{\text{int}}}(0) \rangle}{N_{\text{threshold}} - \langle N_{r_{\text{int}}}(0) \rangle}, \quad (2.12)$$

$$\langle N_{r_{\text{int}}}(t) \rangle = \sum_{j=1}^{N_{A-B}} \frac{N_{r_{\text{int}}}(j, t)}{N_{A-B}}. \quad (2.13)$$

$N_{r_{\text{int}}}$  is the number of solute molecules ( $A - B$ ) present in a circle of radius  $r_{\text{int}}$  for the  $j$ th molecule and  $N_{\text{threshold}}$  is the maximum number of molecules allowed inside it. In order to extract out the dynamical contribution to the order parameter we subtract  $\langle N_{r_{\text{int}}}(0) \rangle$ , from both numerator and denominator. A low nonzero value of  $\psi$  indicates that the number of solute molecules forming the cluster within a circle of radius  $r_{\text{int}}$  on average is much smaller compared to  $N_{\text{threshold}}$ , a situation which conforms more to uniform distribution. On the other hand when  $\psi$  is large and close to unity the solute molecules tend to accommodate themselves within the radius of interaction and to attain a value close to  $N_{\text{threshold}}$  on average. Thus an order parameter close to unity corresponds to the dominance of the clustered state or a state of broken symmetry.

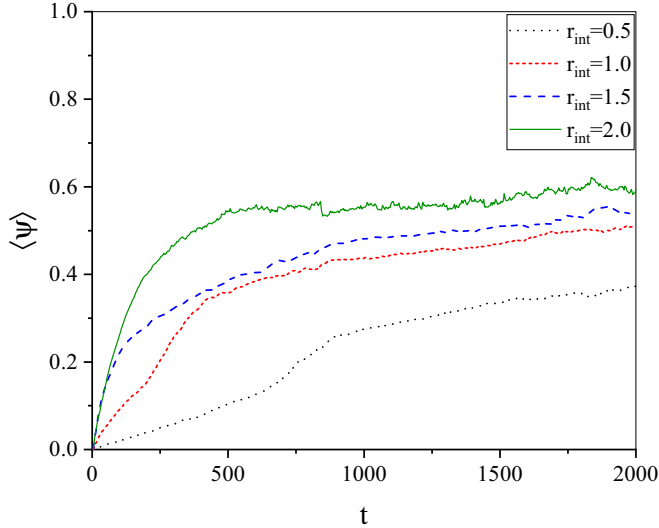


FIG. 3. Plot of the order parameter of the system averaged over 50 mutually independent trajectories vs time for different radii of interaction ( $r_{\text{int}}$ ) simulated with the following parameter values:  $r_{A-B} = 0.3$ ,  $L = 10.0$ ,  $\gamma = 0.5$ ,  $k_B = 1.0$ ,  $T = 1.0$ ,  $N_{A-B} = 100$ ,  $N_C = 1000$ ,  $N_{\text{threshold}} = 20$ ,  $\Delta t = 0.005$  (units arbitrary).

### III. NUMERICAL SIMULATIONS: SYMMETRY BREAKING AND CLUSTERIZATION

The model of the two component solvent-solute system described in the last section is subjected to numerical simulations. The dynamics is followed by monitoring the Brownian motion of solvent particles and self-propelled active motion of solute molecules by generating Gaussian white noise using the Box-Muller algorithm as well as noise with uniform distribution between zero and unity. The time evolution is followed in discrete time steps for the following parameter set for the system with  $N_C = 1000$ ,  $N_{A-B} = 100$ ,  $N_{\text{threshold}} = 20$ ,  $L = 10.0$ ,  $\gamma = 0.5$ ,  $r_{A-B} = 0.3$ ,  $\Delta t = 0.005$ . The Boltzmann constant is set equal to unity. Equilibration of the bath is ensured by monitoring  $\langle v^2 \rangle$  until it reaches the value of the temperature  $T$ . The typical configurations of the position of the self-propelled solute molecules are displayed for  $r_{\text{int}} = 1.0$  and  $T = 1.0$  as snapshots at times  $t = 0$ , 1000, and 2000 in Figs. 2(a), 2(b), and 2(c), respectively. It is evident that as time progresses the heads of the solute molecules tend to cluster around solvent particles due to the affinity between them. This leads to the emergence of some order in the system resulting in symmetry breaking and clusterization.

As a measure of the overall bias of the system towards a symmetry-broken state of clusterization we have shown the variation of order parameter  $\psi$  as a function of time in Fig. 2(d) for the same parameter set and for a single scan over time. The variation exhibits a noisy growth of  $\psi$  from a low value to a relatively high value.

The radius of interaction  $r_{\text{int}}$  plays a crucial role in determining the bias of the system towards the dominance of the clusterized state. As a single scan over time is characteristically noisy, we have plotted the average of the order parameter  $\langle \psi \rangle$  against time over 50 mutually independent scans for several values of  $r_{\text{int}}$  but for the same parameter set in Fig. 3.

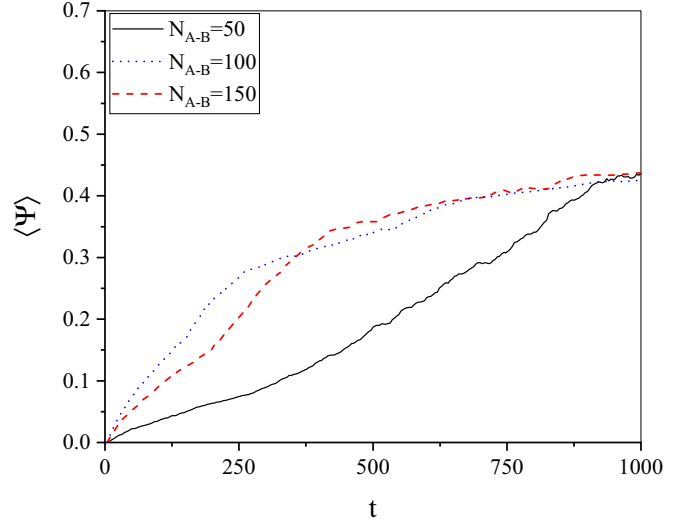


FIG. 4. Plot of the order parameter of the system averaged over 50 mutually independent trajectories vs time for three different numbers of solute molecules simulated with the following parameter values:  $r_{\text{int}} = 2.0$ ,  $r_{A-B} = 0.3$ ,  $L = 10.0$ ,  $\gamma = 0.5$ ,  $k_B = 1.0$ ,  $N_{A-B} = 100$ ,  $N_C = 1000$ ,  $N_{\text{threshold}} = 20$ ,  $\Delta t = 0.005$  (units arbitrary).

For low values of  $r_{\text{int}}$  the local interaction is not sufficient enough to induce any significant bias towards the formation of clusters even in the long time limit. However, when  $r_{\text{int}}$  is increased, one observes a clear dominance of clusters rather than homogeneity as  $\langle \psi \rangle$  converges to a higher value over a time scale  $t = 2000$ .

The phase behavior of active suspension of active systems, particularly of colloids, has often been found to depend on densities [30,31]. Keeping in view these experimental studies we have explored the time evolution of phase behavior in terms of order parameter at several densities. The results are displayed in Fig. 4. It has been observed that for a given  $N_{\text{threshold}}$  and interaction radius  $r_{\text{int}}$  density facilitates the growth of clusters and the approach to stationarity in the long time limit. This can be rationalized in view of the fact that at higher density of solute molecules the probability of finding another molecule gets enhanced within a given radius of interaction.

An important control parameter for the study of coordinated motion in active media such as bird flocks, fish schools, or bacterial swarms is the strength of external noise [1]. In the present investigation we are concerned with an equilibrium bath of solvent particles kept at a constant temperature. The underlying noise is internal, which satisfies the fluctuation-dissipation relationship. It would seem therefore that temperature may serve as a control parameter for our case. To this end we have performed the simulations at five different temperatures for the same set of parameter values. The results are shown in Fig. 5(a), which depicts the variation of the order parameter averaged over 50 mutually independent scans as a function of time. At a very low temperature the average order parameter grows almost linearly up to a time beyond which it reaches a large saturation level. As the temperature is increased the saturation takes place more quickly, the saturation value in the long time limit being lower for higher

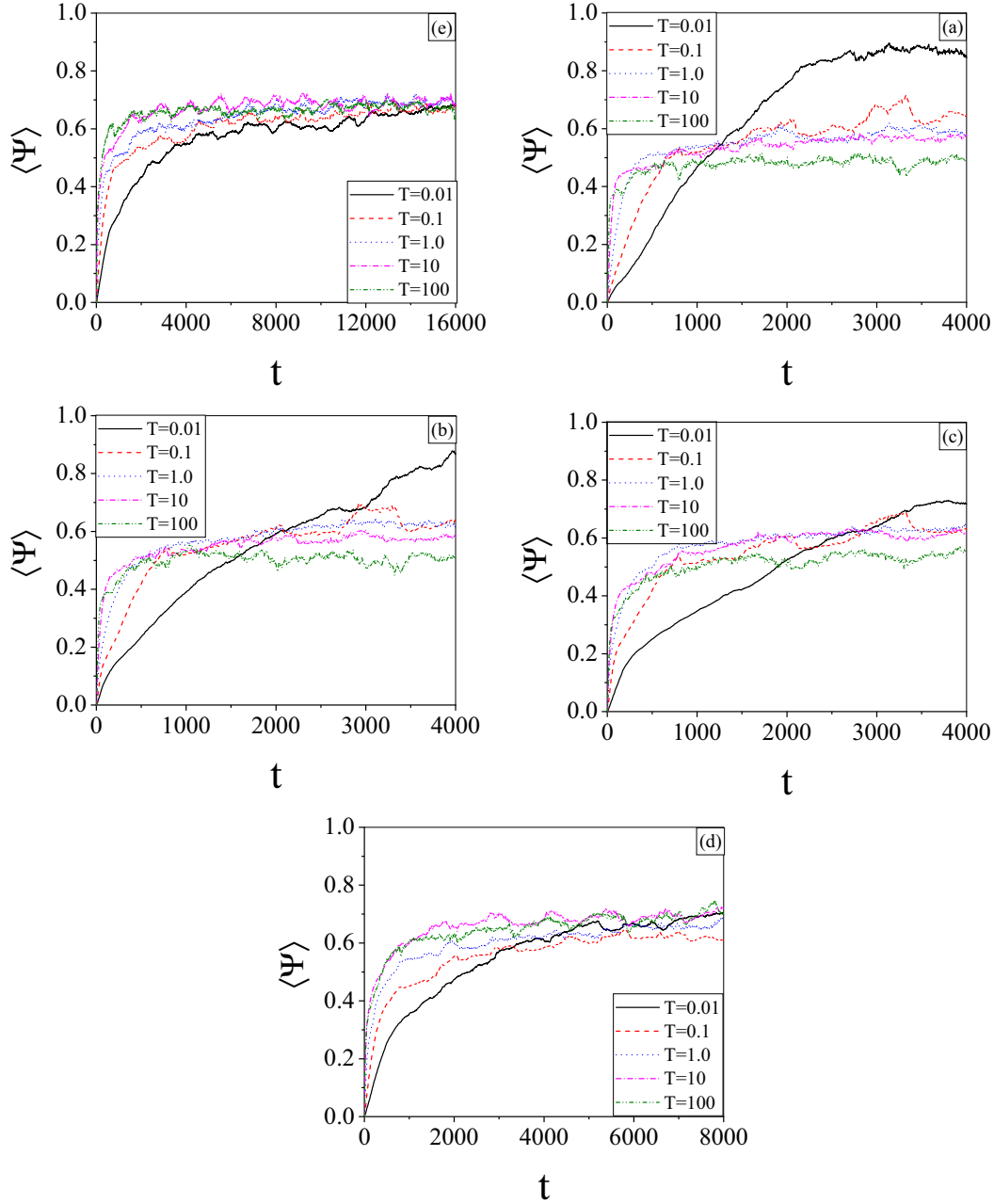


FIG. 5. Plot of the order parameter of the system averaged over 50 mutually independent trajectories vs time for five different temperatures ( $T$ ) using five different  $N_{\text{threshold}}$  values (a)  $N_{\text{threshold}} = 20$ , (b)  $N_{\text{threshold}} = 22$ , (c)  $N_{\text{threshold}} = 24$ , (d)  $N_{\text{threshold}} = 36$ , and (e)  $N_{\text{threshold}} = 40$  simulated with the following parameter values:  $r_{\text{int}} = 2.0$ ,  $r_{A-B} = 0.3$ ,  $L = 10.0$ ,  $\gamma = 0.5$ ,  $k_B = 1.0$ ,  $N_{A-B} = 100$ ,  $N_C = 1000$ ,  $\Delta t = 0.005$  (units arbitrary).

temperature. The effect of temperature is also pronounced through the larger fluctuation in the order parameter curves appearing for higher and higher temperatures. The variation of average order parameter in time for several values of temperature exhibits a crossover at some intermediate time. Below this time temperature enhances clusterization, whereas lowering of temperature favors clusterization in the long time limit. It is also important to note that for a fixed  $N_{\text{threshold}}$  which is not large  $\langle \psi \rangle$  never reaches unity. This implies that there always exists a finite number of free solute molecules which are in dynamic equilibrium with the cluster phase.

To understand the role of  $N_{\text{threshold}}$  on the crossover time we have performed numerical simulations for different  $N_{\text{threshold}}$  values and the results are plotted in Fig. 5. The  $N_{\text{threshold}}$  value is gradually increased from Fig. 5(a) to Fig. 5(e). It is evident that the crossover time is indeed dependent on the  $N_{\text{threshold}}$  value. With increase in  $N_{\text{threshold}}$  value, the crossover time increases steadily, and finally for a very high value of  $N_{\text{threshold}}$  the crossover phenomenon completely disappears. To explain this absence of crossover at high  $N_{\text{threshold}}$  value we proceed as follows: we first find out the maximum possible value of  $N_{\text{threshold}}$  ( $N_{\text{threshold}}^{\text{max}}$ ). A simple estimate of  $N_{\text{threshold}}^{\text{max}}$  in

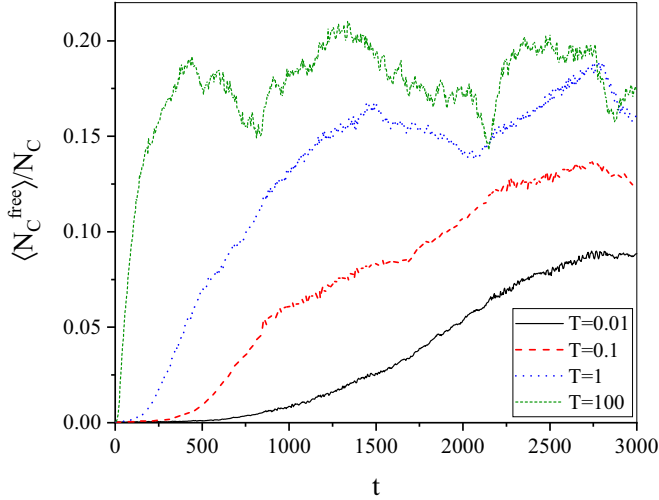


FIG. 6. Plot of  $\frac{N_C^{\text{free}}}{N_C}$  averaged over 50 mutually independent trajectories vs time for four different temperatures ( $T$ ) simulated with the following parameter values:  $r_{\text{int}} = 2.0$ ,  $r_{A-B} = 0.3$ ,  $L = 10.0$ ,  $\gamma = 0.5$ ,  $k_B = 1.0$ ,  $N_{A-B} = 100$ ,  $N_C = 1000$ ,  $N_{\text{threshold}} = 20$ ,  $\Delta t = 0.005$  (units arbitrary).

two dimensions can be defined as

$$N_{\text{threshold}}^{\text{max}} = \frac{4\pi r_{\text{int}}^2}{4\pi r_{A-B}^2} = \left( \frac{r_{\text{int}}}{r_{A-B}} \right)^2. \quad (3.1)$$

Now for the parameter values used in our calculation, i.e.,  $r_{\text{int}} = 2.0$  and  $r_{A-B} = 0.3$ , the  $N_{\text{threshold}}^{\text{max}}$  is roughly equal to 44. As the value of  $N_{\text{threshold}}$  approaches the  $N_{\text{threshold}}^{\text{max}}$  value the crossover tends to disappear because the number of free solute molecules present in the system is inversely proportional to the  $N_{\text{threshold}}$  value; at the higher limit there remain a very few solute molecules which can be further accommodated in the already formed clusters to further enhance the order parameter, and as a result the order parameter saturates to a constant value with small temporal fluctuations. The value of  $N_{\text{threshold}}^{\text{max}}$  is dependent on radius of interaction ( $r_{\text{int}}$ ) and radius of solute molecules ( $r_{A-B}$ ) whereas the  $N_{\text{threshold}}$  value is independent of such parameters. To stress the physical meaning of  $N_{\text{threshold}}^{\text{max}}$  and  $N_{\text{threshold}}$  we may treat  $N_{\text{threshold}}$  as a quantity analogous to the coordination number ( $\phi$ ) of a chemical system. For chemical systems the coordination number is the number of ligands that surround a central metal atom to form a coordination complex, and this number explicitly depends on the chemical property of both the metal and ligand; furthermore the coordination number cannot exceed  $\phi_{\text{max}}$ , which is dependent on the size of the metal and ligand. In our model we have considered the solvent particles and solute molecules on a general footing without being concerned about the details of their chemical property. This leads us to choose the value of  $N_{\text{threshold}}$  such that it does not exceed  $N_{\text{threshold}}^{\text{max}}$ , which is determined by the parameters of the system. The assistance of clusterization by temperature below the crossover time can be understood further from a quasithermodynamic consideration. To highlight this issue we have calculated the number of free solvent particles present ( $N_C^{\text{free}}$ ) at any time out of total solvent particles ( $N_C$ ) and plotted in Fig. 6 the variation of the

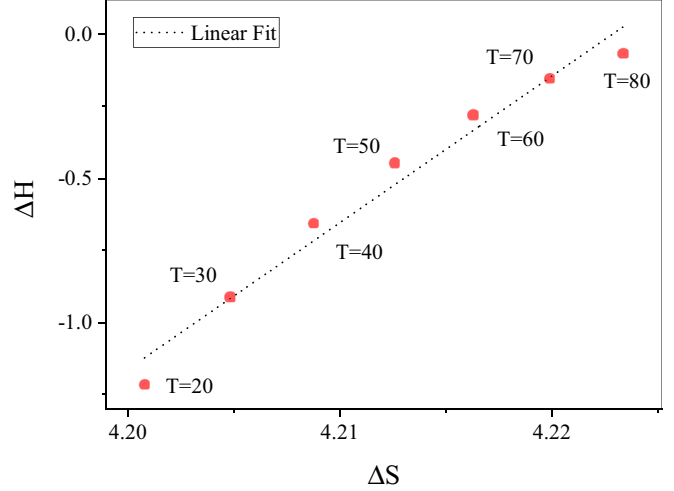


FIG. 7. Plot of  $\Delta H$  vs  $\Delta S$  for the parameter set mentioned in the text (units arbitrary).

ratio  $\frac{N_C^{\text{free}}}{N_C}$  against time, averaged over 50 independent scans for the parameter set used in Fig. 5. Here the free solvent particle is defined as the solvent particle for which there is no solute molecule present within the radius of interaction  $r_{\text{int}}$ . Since the free solvent particles essentially guide the entropy of the system, the plots show that for higher temperature the change in entropy is more positive. Furthermore, the clusterization is exothermic in nature. Therefore for positive entropy change and negative enthalpy change increase in temperature assists the thermodynamically favorable process of clusterization below the crossover time. We shall return to an enthalpy-entropy relation in a more quantitative way in the next section. Finally we note that beyond the crossover time the quasithermodynamic nature of the system through self-propulsion dominates the scenario, where the lowering of temperature assists clusterization, giving rise to higher saturation value of the order parameter. Thus although in general the system is quasithermodynamic in character, below the crossover time temperature helps in fast thermalization and clusterization.

#### IV. CLUSTERIZATION: ENTHALPY-ENTROPY COMPENSATION

As the process of flocking leading to self-assembly of solute molecules  $A - B$  around solvent particles  $C$  is governed by both attractive and repulsive interactions within a given domain, it is imperative that enthalpic and entropic changes play significant roles in clusterization. It is particularly interesting to enquire how the balance of the two interactions influences clusterization so that the self-assemblies remain robust against perturbation. This phenomenon of enthalpy-entropy compensation is widely invoked in thermodynamic analysis of proteins, ligands, and nucleic acids. It has been suggested that this compensation is an intrinsic property of complex, fluctuating systems undergoing associative processes. The enthalpy-entropy compensation phenomenon has been studied theoretically as well as experimentally [49–51] in several contexts.

In general, the compensation between the standard enthalpy change  $\Delta H$  and the standard entropy change  $\Delta S$  in the various associative processes can be described as follows:

$$\Delta H = \alpha + \beta \Delta S. \quad (4.1)$$

In the spirit of the phase separation and the mass action models [52,53], the standard Gibbs free energy of clusterization  $\Delta G$  can be expressed as

$$\Delta G = RT \ln X. \quad (4.2)$$

For the clusterization model described here  $X$  stands for the ratio of average number of solute molecules  $A - B$  per cluster to the total number of solute molecules and solvent particles present in the system, i.e.,

$$X = \frac{\langle \overline{N_{r_{\text{int}}}} \rangle}{N_{A-B} + N_C}. \quad (4.3)$$

Here,  $\langle \overline{N_{r_{\text{int}}}} \rangle$  represents the time average over the ensemble average of  $\langle N_{r_{\text{int}}} \rangle$  for 50 independent trajectories, within the time interval 400 to 500 time units.

To evaluate the enthalpy and entropy of clusterization,  $\ln X$  is correlated by a polynomial equation of the form

$$\ln X = a + bT + cT^2. \quad (4.4)$$

Here,  $a$ ,  $b$ , and  $c$  are the unknown constants to be determined. Making use of the Gibbs-Helmholtz equation, enthalpy change  $\Delta H$

$$\Delta H = -T^2 \frac{\partial(\Delta G/T)}{\partial T} = -RT^2 \frac{\partial(\ln X)}{\partial T} \quad (4.5)$$

and the entropy change of clusterization

$$\Delta S = \frac{1}{T} (\Delta H - \Delta G) \quad (4.6)$$

are determined. We now numerically estimate the variation of  $\ln X$  as a function of temperature over the range from  $T = 20$  to  $80$  for the parameter set  $r_{\text{int}} = 2.0$ ,  $r_{A-B} = 0.3$ ,  $L = 10.0$ ,  $\gamma = 0.5$ ,  $N_{A-B} = 100$ ,  $N_C = 1000$ ,  $N_{\text{threshold}} = 20$ ,  $\Delta t = 0.005$  with  $k_B$  set equal to unity. From the variation of  $\ln X$  as a function of temperature the parameter values as determined by the polynomial fit are  $a = -4.23094$ ,  $b = 1.6063 \times 10^{-4}$ , and  $c = -1.87837 \times 10^{-7}$ .

The use of the expression for  $\ln X$  in Eqs. (4.5) and (4.6) yields  $\Delta H$  and  $\Delta S$ :

$$\Delta H = -RT^2(b + 2cT), \quad (4.7)$$

$$\Delta S = -R(a + 2bT + 3cT^2). \quad (4.8)$$

The value of  $R$  is set to be unity throughout our calculation. In Fig. 7 we have plotted the  $\Delta H$  with respect to  $\Delta S$  using the aforementioned fitting parameters and the temperature range. The  $\Delta H - \Delta S$  plot exhibits approximate linearity, i.e., enthalpy-entropy compensation in our clusterization model. The deviation from strict linearity may be explained as follows: The argument on enthalpy-entropy compensation stems from thermodynamic consideration. The two-component system composed of active solute molecules in passive solvent particles comprising a thermal bath is not strictly thermodynamic because of the orientational fluctuations of active

molecules (of external origin). This is expected particularly for  $N_{\text{threshold}} < N_{\text{threshold}}^{\text{max}}$ . The deviation therefore signifies a quasithermodynamic character of the mixture. A linear fit through the data points results in  $\alpha = -215.04146$  and compensation temperature  $\beta = 50.9234$ . The approximate linearity of the compensation plot signifies that the repulsive interaction between solute molecules forming clusters within  $r_{\text{int}}$  balances the attractive interaction between the solvent particles and the solute molecules. As the repulsion is due to confinement it contributes to free energy of clusterization as the entropy component while the attractive interaction contributes to the enthalpic component. The existence of a compensation temperature is reminiscent of Boyle temperature in a nonideal gas where the attractive and repulsive interactions exactly balance each other.

## V. CONCLUSION

In this paper we have investigated a solvent-solute two-component system to examine the active dynamics of solute molecules suspended in a thermal bath of solvent particles. The activity originates from the chemical affinity of one of the heads of the solute molecules towards solvent particles. The time evolution of the dynamics is essentially controlled by two factors: first, the interaction between solute heads and solvent particles within a specified range, and second, temperature of the thermal bath since it governs the mean speed of the active solute molecules. No specific form of interaction potential is chosen for the purpose and in this sense the spirit of the approach conforms to that of the Vicsek model. We have observed that for an optimal range of interaction radius the active solute molecules undergo formation of a clustered phase in dynamic equilibrium with free solute molecules. The role of temperature is twofold. First, temperature assists clustering up to a crossover time, an observation consistent with thermodynamics of entropy increase of free solvent particles. In other words, clusterization is favored by fast thermalization due to high temperature as observed below the crossover time, while active motion is facilitated at lower temperature beyond the crossover where the quasithermodynamic regime dominates. Second, the temperature dependence of clusterization used to calculate the enthalpy and entropy changes shows a rough balance between the attractive interaction between the two components due to their affinity, and the repulsive interaction due to confinement of one of the components forming the clusters within an interaction regime, which is manifested through enthalpy-entropy compensation. The deviation from strict linearity of the compensation plot is indicative of the fact that the statistical behavior of mixing active molecules in a thermal suspension of solute particles is quasithermodynamic rather than thermal in character. We believe that the present numerical exploration can be useful for understanding formation of chemotactic aggregates in bacterial populations [54,55].

## ACKNOWLEDGMENTS

Thanks are due to the University Grants Commission, Government of India for a fellowship (S.P.) and

Department of Science and Technology, under Government of India, for a J. C. Bose National Fellowship (D.S.R.)

under Grant No. SB/S2/JCB-030/2015 for partial financial support.

- [1] T. Vicsek, A. Czirók, E. Ben-Jacob, I. Cohen, and O. Shochet, *Phys. Rev. Lett.* **75**, 1226 (1995).
- [2] H. Chaté, F. Ginelli, G. Grégoire, F. Peruani, and F. Raynaud, *Eur. Phys. J. B* **64**, 451 (2008).
- [3] J. Toner and Y. Tu, *Phys. Rev. Lett.* **75**, 4326 (1995).
- [4] J. Toner and Y. Tu, *Phys. Rev. E* **58**, 4828 (1998).
- [5] R. A. Simha and S. Ramaswamy, *Phys. Rev. Lett.* **89**, 058101 (2002).
- [6] K. Kruse, J. F. Joanny, F. Jülicher, J. Prost, and K. Sekimoto, *Eur. Phys. J. E* **16**, 5 (2005).
- [7] T. Vicsek and A. Zafeiris, *Phys. Rep.* **517**, 71 (2012).
- [8] M. C. Marchetti, J. F. Joanny, S. Ramaswamy, T. B. Liverpool, J. Prost, M. Rao, and R. A. Simha, *Rev. Mod. Phys.* **85**, 1143 (2013).
- [9] B. Sabass and U. Seifert, *J. Chem. Phys.* **136**, 064508 (2012).
- [10] P. K. Ghosh, Y. Li, G. Marchegiani, and F. Marchesoni, *J. Chem. Phys.* **143**, 211101 (2015).
- [11] D. Debnath, P. K. Ghosh, Y. Li, F. Marchesoni, and B. Li, *J. Chem. Phys.* **145**, 191103 (2016).
- [12] T. Feder, *Phys. Today* **60**(1), 28 (2007).
- [13] S. Hubbard, P. Babak, S. Th. Sigurdsson, and K. G. Magnússon, *Ecol. Modell.* **174**, 359 (2004).
- [14] E. M. Rauch, M. M. Millonas, and D. R. Chialvo, *Phys. Lett. A* **207**, 185 (1995).
- [15] E. Ben-Jacob, I. Cohen, O. Shochet, A. Tenenbaum, A. Czirók, and T. Vicsek, *Phys. Rev. Lett.* **75**, 2899 (1995).
- [16] W. J. Rappel, A. Nicol, A. Sarkissian, H. Levine, and W. F. Loomis, *Phys. Rev. Lett.* **83**, 1247 (1999).
- [17] D. Helbing, J. Keltsch, and P. Molnár, *Nature (London)* **388**, 47 (1997).
- [18] G. Grégoire and H. Chaté, *Phys. Rev. Lett.* **92**, 025702 (2004).
- [19] Z. Csahók and A. Czirók, *Physica A* **243**, 304 (1997).
- [20] V. Schaller, C. Weber, C. Semmrich, E. Frey, and A. R. Bausch, *Nature (London)* **467**, 73 (2010).
- [21] F. C. Keber, E. Loiseau, T. Sanchez, S. J. DeCamp, L. Giomi, M. J. Bowick, M. C. Marchetti, Z. Dogic, and A. R. Bausch, *Science* **345**, 1135 (2014).
- [22] J. Ranft, M. Basan, J. Elgeti, J. F. Joanny, J. Prost, and F. Jülicher, *Proc. Natl. Acad. Sci. USA* **107**, 20863 (2010).
- [23] M. Basan, T. Risler, J. F. Joanny, X. Sastre-Garau, and J. Prost, *HFSP J.* **3**, 265 (2009).
- [24] D. Bhattacharyya, S. Paul, S. Ghosh, and D. S. Ray, *Phys. Rev. E* **97**, 042125 (2018).
- [25] S. Paul, S. Ghosh, and D. S. Ray, *Phys. Rev. E* **97**, 022213 (2018).
- [26] J. Palacci, S. Sacanna, A. P. Steinberg, D. J. Pine, and P. M. Chaikin, *Science* **339**, 936 (2013).
- [27] Y. L. Chen and H. R. Jiang, *Appl. Phys. Lett.* **109**, 191605 (2016).
- [28] I. Buttinoni, J. Bialké, F. Kümmel, H. Löwen, C. Bechinger, and T. Speck, *Phys. Rev. Lett.* **110**, 238301 (2013).
- [29] F. B. Usabiaga, B. Delmotte, and A. Donev, *J. Chem. Phys.* **146**, 134104 (2017).
- [30] X. L. Wu and A. Libchaber, *Phys. Rev. Lett.* **84**, 3017 (2000).
- [31] I. Theurkauff, C. Cottin-Bizonne, J. Palacci, C. Ybert, and L. Bocquet, *Phys. Rev. Lett.* **108**, 268303 (2012).
- [32] P. K. Ghosh, V. R. Misko, F. Marchesoni, and F. Nori, *Phys. Rev. Lett.* **110**, 268301 (2013).
- [33] X. Ao, P. K. Ghosh, Y. Li, G. Schmid, P. Hänggi, and F. Marchesoni, *Eur. Phys. J. Spec. Top.* **223**, 3227 (2014).
- [34] P. K. Ghosh, P. Hänggi, F. Marchesoni, and F. Nori, *Phys. Rev. E* **89**, 062115 (2014).
- [35] X. Ao, P. K. Ghosh, Y. Li, G. Schmid, P. Hänggi, and F. Marchesoni, *Europhys. Lett.* **109**, 10003 (2015).
- [36] Z. Liu, L. Du, W. Guo, and D. C. Mei, *Eur. Phys. J. B* **89**, 222 (2016).
- [37] M. Tarama and T. Ohta, *Eur. Phys. J. B* **83**, 391 (2011).
- [38] P. K. Ghosh, *J. Chem. Phys.* **141**, 061102 (2014).
- [39] J. R. Howse, R. A. L. Jones, A. J. Ryan, T. Gough, R. Vafabakhsh, and R. Golestanian, *Phys. Rev. Lett.* **99**, 048102 (2007).
- [40] J. Palacci, C. Cottin-Bizonne, C. Ybert, and L. Bocquet, *Phys. Rev. Lett.* **105**, 088304 (2010).
- [41] G. Miño, T. E. Mallouk, T. Darnige, M. Hoyos, J. Dauchet, J. Dunstan, R. Soto, Y. Wang, A. Rousselet, and E. Clement, *Phys. Rev. Lett.* **106**, 048102 (2011).
- [42] E. F. Semeraro, J. M. Devos, and T. Narayanan, *J. Chem. Phys.* **148**, 204905 (2018).
- [43] J. Grabowska, A. Kuffel, and J. Zielkiewicz, *J. Chem. Phys.* **147**, 174502 (2017).
- [44] M. B. Sweatman and L. Lue, *J. Chem. Phys.* **144**, 171102 (2016).
- [45] H. Noguchi and G. Gompper, *Phys. Rev. Lett.* **93**, 258102 (2004).
- [46] E. Allahyarov and G. Gompper, *Phys. Rev. E* **66**, 036702 (2002).
- [47] M. Ripoll, K. Mussawisade, R. G. Winkler, and G. Gompper, *Phys. Rev. E* **72**, 016701 (2005); A. Malevanets and R. Kapral, *J. Chem. Phys.* **112**, 7260 (2000).
- [48] A. Malevanets and R. Kapral, *J. Chem. Phys.* **110**, 8605 (1999); R. G. Winkler, K. Mussawisade, M. Ripoll, and G. Gompper, *J. Phys.: Condens. Matter* **16**, S3941 (2004).
- [49] L. J. Chen, S. Y. Lin, and C. C. Huang, *J. Phys. Chem. B* **102**, 4350 (1998).
- [50] E. Grunwald and C. Steel, *J. Am. Chem. Soc.* **117**, 5687 (1995).
- [51] J. F. Douglas, J. Dudowicz, and K. F. Freed, *Phys. Rev. Lett.* **103**, 135701 (2009).
- [52] E. Matijević and B. A. Pethica, *Trans. Faraday Soc.* **54**, 587 (1958).
- [53] J. N. Phillips, *Trans. Faraday Soc.* **51**, 561 (1955).
- [54] E. O. Budrene and H. C. Berg, *Nature (London)* **376**, 49 (1995).
- [55] F. Keller and L. A. Segel, *J. Theor. Biol.* **26**, 399 (1970).